

# Predictive Model for Oil Reservoirs in the Niger Delta Under Xanthan Polymer Flooding

Daniel Oji Ndem

Department of Petroleum and Gas Engineering, *Federal University Otuoke, Bayelsa*

doi: <https://doi.org/10.37745/ijeats.13/vol13n3119>

Published June 29, 2025

**Citation:** Ndem D.O. (2025) Predictive Model for Oil Reservoirs in the Niger Delta Under Xanthan Polymer Flooding, *International Journal of Engineering and Advanced Technology Studies*, 13 (3), 1-19

**Abstract:** *This study developed a mathematical model to evaluate the effectiveness of Xanthan polymer flooding in enhancing oil recovery from Niger Delta reservoirs with low oil viscosity and homogeneous temperature based on the polymer solution viscosity which is a direct function of polymer concentration. Experimental results showed that increasing polymer concentration from 200mg/L to 1000mg/L increases the polymer solution viscosity and thereby improves oil recovery. The developed model predicted optimal oil recovery of 127.5 MMm<sup>3</sup> at a polymer concentration of 600mg/L, with a percentage error of 2.91% when validated by the Buckley-Leverett model. The results demonstrate the importance of optimizing Xanthan polymer concentration for efficient oil recovery through a simple predictive model.*

**Keywords;** polymer flooding, polymer solution concentration, mathematical model, cumulative oil recovery

## INTRODUCTION

The efficiency of xanthan gum polymer flooding in enhancing oil recovery is significantly influenced by the viscosity of the polymer solution, which in turn is a function of several parameters such as polymer concentration, temperature, and salinity [1], [2]. As a biopolymer, xanthan gum offers a promising alternative to traditional polyacrylamide-based polymers, with its unique rheological properties and environmental benefits. The design of optimal xanthan gum polymer concentration for field programs requires careful consideration of reservoir conditions, practicality, and the complex interactions between the polymer solution, rock, and fluid properties [3].

By understanding these factors, xanthan gum polymer flooding can be optimized to improve oil recovery and reduce the environmental footprint of enhanced oil recovery. Numerous mathematical models have been developed to analyze the performance of polymer injection in enhanced oil

recovery (EOR) operations. For instance, a simplified mathematical model was proposed to evaluate the effectiveness of polymer flooding, assuming a negligible impact of polymer concentration on the process [4]. In another study, an empirical model leveraging artificial neural networks was employed to forecast oil recovery during polymer flooding assisted by nanofluids. The results indicated that the hybrid approach yielded an additional 18% oil-in-place recovery, with a moderate error of 8.7% between predicted and actual values [5]. Furthermore, a comprehensive investigation utilized the Buckley-Leverett predictive model to generate a large dataset (over 163,000 samples) encompassing diverse reservoir conditions. This dataset was subsequently used to train and evaluate seven machine learning models and two neural network models, aiming to predict the oil recovery factor based on seven input parameters. The findings revealed that a polynomial regression-based model achieved a coefficient of determination ( $R^2$ ) of 0.909, demonstrating its reliability in predicting oil recovery factors [6].

Recent studies have demonstrated the efficacy of polymer flooding in enhancing oil recovery from complex reservoirs. For instance, a machine-assisted reservoir simulation model was developed to forecast oil recovery from the Alaska North Slope field, a high-viscosity oil reservoir [7]. The simulation incorporated viscous fingering to account for the inefficient water flooding operations, and the results indicated that polymer flooding yielded higher oil recovery rates compared to water flooding. The UTCHEM reservoir simulator has undergone significant enhancements, incorporating new physical property models to bolster its predictive capabilities for polymer flooding applications. Notably, an advanced polymer viscosity model has been integrated, enabling accurate viscosity calculations as a function of concentration, shear rate, salinity, and temperature. Furthermore, a hydrolysis model and a cation exchange model have been incorporated to facilitate the selection of suitable polymers for specific reservoir conditions [8].

The validity of these new models has been established through rigorous validation using high-quality laboratory data, and their application has been demonstrated through simulation cases that upscale laboratory results to field-scale scenarios. The updated inaccessible pore volume model is particularly noteworthy, as it enables the selection of reservoir-compatible polymers and enhances the accuracy of simulations. These enhancements to the UTCHEM simulator are anticipated to significantly improve the design and optimization of polymer flooding applications, ultimately leading to more efficient and effective oil recovery [9].

Polymer flooding has emerged as a widely adopted method for Enhanced Oil Recovery (EOR), and its effectiveness can be attributed to various factors. A comprehensive review of the current state of polymer flooding highlights the dominance of Hydrolyzed Polyacrylamide (HPAM) as the preferred polymer, while also discussing the challenges and opportunities for alternative polymers and mobility-control methods [10]. Notably, the review emphasizes the importance of designing the injected polymer viscosity and the need for large polymer banks to optimize oil recovery.

Recent studies have revealed that polymer visco-elasticity plays a crucial role in mobilizing residual oil and improving microscopic displacement efficiency, thereby enhancing oil recovery [11]. However, the application of polymer flooding in carbonates is limited due to extreme reservoir conditions, such as high temperatures and salinity. To overcome these challenges, novel polymers with unique monomers have been developed to protect them from chemical and thermal degradation [12].

Mathematical modeling has also been employed to investigate the effects of polymer flooding on oil recovery. A displacement mathematical model based on Buckley-Leverett theory was developed to study the changes in water saturation during polymer solution injection [13]. The results showed that water saturation decreases during flow due to oil phase accumulation in the porous medium, and the rate of change in water saturation remains constant when the oil viscosity is 70 mPa·s and water-oil mobility ratio is 0.4.

Furthermore, core samples experiments have been conducted to develop mathematical models that consider the influences of temperature, salinity, polymer concentration, and dispersion on oil recovery [14]. These models provide valuable insights into the complex interactions between polymer flooding and oil recovery, enabling the optimization of EOR operations.

A predictive model was developed by taking into consideration the polymer concentration to derive the polymer viscosity at zero shear rate ( $\mu_p^0$ ). The model presented the viscosity of polymer at zero shear rate as a function of salinity, polymer concentration, and water viscosity

$$\mu_p^0 = \mu_w [1 + (a_1 c_p + a_2 c_p^2 + a_3 c_p^3) c_s^{sp}]. \quad [15]$$

A combination of experimental and simulation experiment was studied to develop a black oil mathematical model for oil and water systems that can be used to evaluate polymer flooding. The model consists of non-homogeneous, nonlinear simultaneous partial differential equations.[16]

Evaluating the effect of polymer concentration, rate of viscous fingering growth during constant temperature polymer flooding process led to the development of a model. The result indicated that the saturation of residual oil decreases for high polymer concentration. The model relates the adsorbed polymer concentration to the maximum adsorbed polymer concentration, polymer concentration, and polymer adsorption coefficient.[17]

$$c_{ap} = c_{ap} \max (b_p c_p / 1 + b_p c_p)$$

A mathematical model that estimates pressure differentials and studies the efficiency of polymer flooding by considering the effects of heterogeneity, plugging of reservoir, and fluid saturation has been developed.[18]

Consideration of the effect of elasticity of polymer solution viscosity in residual oil recovery was studied, and used to evaluate the influences of injection rate, salinity polymer molecular weight well space and degradation rate on oil recovery in developing a model to predict the changes in

viscosity of polymer solution during polymer flooding as a function of shear rate, water viscosity, and polymer viscosity at zero shear rate the model is given as:

$$\mu_{ps} = \mu_w + (\mu_p^0 - \mu_w) / [1 + (\gamma_e / \gamma_{1/2})^{a-1}]. \quad [19]$$

Evaluation of micro displacement simulations to establish a model that can estimate in-situ rheology by varying rock power index of the Carreau model before introducing correction factor was analyzed. A linear function was introduced between apparent shear rate, darcy velocity, and the correction factor. The results showed that the major influencing factors of in-situ polymer solution viscosity are the remote pore volume of the rock, and the pore aspect ratio.[20]

A two-dimensional multi-phase compositional polymer injection model in both homogeneous and non-homogeneous petroleum reservoirs based on a streamline approach was developed by applying the implicit pressure and explicit saturation method to estimate pressure and fluid saturation in the black oil system.[21] An incorporation of simulation, and laboratory tests to study polymer injection in heavy oil reservoirs associated with heterogeneity was investigated. From the investigation, a mathematical model was developed to analyze polymer degradation; shear thinning of polymer solution and non-Newtonian flow in heterogeneous porous media and the results revealed that these factors adversely influence the polymer flooding efficiency.[22]

An oil recovery prediction model that is dependent on the stream tube theory was generated, the research established an areal sweep efficiency equation appropriate for a rhombus inverse nine-spot well flooding pattern based on the proposition that the stream tube between injection and production wells is trapezoidal. The model was able to predict an oil recovery of 1.37 % against the actual field recovery of 1.22 %, this result established that oil recovery is inversely proportional to injection rate, injection concentration , and polymer micro-spheres.[23]

## MATERIALS AND METHODS

The following materials and apparatuses were used in this research: Xanthan gum, weighing pan, brine water, beakers, thermometer, spatula, viscometer, weighing scale.

### Methods

Polymer solutions were formulated with different weights of Xanthomonas Campestris commercial referred to as xanthan. The weights ranging from 200mg to 1000mg as measured with a scale were dissolved respectively in one litre of brine water with a salinity of 2000 ppm contained in various beakers. These formulations were heated to 80c and stirred vigorously with a spatula. The viscosity of the polymer solutions formulated were measured with a digital rotational viscometer. With reservoir data and relative permeability data, fractional flow theory was applied, followed by [24] to calculate the cumulative oil recovery at each polymer solution concentration. Finally, regression analysis was applied to develop a mathematical model for the estimation of cumulative oil recovery from reservoirs containing oil with a viscosity range of 1centipoise to 100 centipoises.

Table 1(a) Reservoir Data

Reservoir width	2350m
Reservoir Length	4375m
Porosity	20%
Reservoir temperature °F	140 °F – 176°F
Formation dip angle (degrees)	0
Reservoir average permeability	150md
Connate water	41%
Oil viscosity	10 cp
Water viscosity	0.5 cp
Oil formation volume factor	1.01
Water formation volume factor	1.0

Table 1(b) Relative Permeability Data

Sw	0.410	0.503	0.530	0.558	0.585	0.640	0.668	0.695	0.723	0.750
Kro	1.000	0.812	0.643	0.493	0.364	0.163	0.092	0.041	0.010	0.000
Krw	0.000	0.003	0.012	0.025	0.044	0.095	0.127	0.164	0.205	0.251

Considering the reservoir data of Table (1a) and (1b), fractional flow theory was applied to calculate the fractional flow of polymer solution and oil using;

$$F_p = \frac{1}{1 + \left(\frac{k_{rpo}}{k_{rw}\mu_o}\right)} \dots\dots\dots 1$$

The viscosity of the polymer solution was substituted in the fractional flow equation to derive the fractional flow of the polymer solution, which was calculated for the various polymer viscosity.

### Application of Buckley Leverett and Welge Tangent Method

Then Buckley-Leverett and Welge's tangent method was applied to determine the cumulative oil production after the polymer solution breakthrough. The oil recoveries calculated from the Buckley-Leverett and Welge tangent method were applied to the various polymer solution viscosity corresponding to the polymer concentration using;

$$N_p = \frac{AL\phi(S_{wb} - S_{wc})}{Bo} \dots\dots\dots 2$$

Equation 2 was applied in the calculation of the cumulative oil production after the breakthrough of polymer solution, the water saturation at breakthrough  $S_{wb}$  was determined by plotting the values of the fractional flow of polymer solution ( $F_p$ ) against water saturation values ( $S_w$ ).

The graph of  $F_p$  versus  $S_w$  gave an S-curve, by drawing a tangent from the connate water value to the  $F_p$  at unity, the value of  $S_{wbt}$  was traced. This process was carried out for the viscosity of each polymer solution fractional flow ( $F_p$ ).

#### **$N_p$ at $F_p$ of 6 centipoises**

Breakthrough saturation  $S_{wbt} = 0.735$

Connate water saturation = 0.410

Porosity = 20%

$$\text{Cumulative oil production after breakthrough (Np)} = \frac{179 * 2350 * 4375 * 0.2 * 0.325}{1.01} = 118,437,964.11 = 118.44 \text{ MM m}^3$$

#### **$N_p$ at $F_p$ of 15 centipoises**

Breakthrough saturation  $S_{wbt} = 0.745$

Connate water saturation = 0.410

Porosity = 20%

$$\text{Cumulative oil production after breakthrough (Np)} = \frac{179 * 2350 * 4375 * 0.2 * 0.335}{1.01} = 122,082,209.16 = 122.08 \text{ MM m}^3$$

#### **$N_p$ at $F_p$ of 18.7 centipoise**

Breakthrough saturation  $S_{wbt} = 0.749$

Connate water saturation = 0.410

Porosity = 20%

$$\text{Cumulative oil production after breakthrough (Np)} = \frac{179 * 2350 * 4375 * 0.2 * 0.339}{1.01} = 123,539,907.18 = 123.54 \text{ MM m}^3$$

#### **$N_p$ at $F_p$ of 22 centipoises**

Breakthrough saturation  $S_{wbt} = 0.750$

Connate water saturation = 0.410

Porosity = 20%

$$\text{Cumulative oil production after breakthrough (Np)} = \frac{179 * 2350 * 4375 * 0.2 * 0.340}{1.01} \\ = 123,904,331.68 = 123.90 \text{ MM m}^3$$

#### **N<sub>p</sub> at F<sub>p</sub> of 29.5 centipoise**

$$\text{Breakthrough saturation } S_{wbt} = 0.750$$

$$\text{Connate water saturation} = 0.410$$

$$\text{Porosity} = 20\%$$

$$\text{Cumulative oil production after breakthrough (Np)} =$$

$$\frac{179 * 2350 * 4375 * 0.2 * 0.340}{1.01} = 123,904,331.68 = 123.90 \text{ MM m}^3$$

#### **N<sub>p</sub> at F<sub>p</sub> of 37 centipoises**

$$\text{Breakthrough saturation } S_{wbt} = 0.750$$

$$\text{Connate water saturation} = 0.410$$

$$\text{Porosity} = 20\%$$

$$\text{Cumulative oil production after breakthrough (Np)} =$$

$$\frac{179 * 2350 * 4375 * 0.2 * 0.340}{1.01} = 123,904,331.68 = 123.90 \text{ MM m}^3$$

#### **N<sub>p</sub> at F<sub>p</sub> of 51 centipoises**

$$\text{Breakthrough saturation } S_{wbt} = 0.750$$

$$\text{Connate water saturation} = 0.410$$

$$\text{Porosity} = 20\%$$

$$\text{Cumulative oil production after breakthrough (Np)} =$$

$$\frac{179 * 2350 * 4375 * 0.2 * 0.340}{1.01} = 123,904,331.68 = 123.90 \text{ MM m}^3$$

#### **Application of Regression Analysis**

Regression analysis was applied to a plot of polymer solution concentration and Buckley-Leveret calculated cumulative oil production. Polymer solution concentration (Pc) was plotted on the x-axis, and cumulative oil production (Np) on the y-axis.



Calculating the mean of polymer solution and calculated cumulative oil production.

$$\bar{x} \text{ (mean of } P_c) = (200 + 400 + 500 + 600 + 700 + 800 + 1000) / 7 = P_{c1} = 600 \text{ mg}$$

$$\bar{y} \text{ (mean of } N_p) = (118.44 + 122.08 + 123.54 + 123.9 + 123.9 + 123.9 + 123.9) / 7 \\ = N_{p1} = 122.81 \text{ m}^3$$

Calculating the sum of the products of the differences from the mean of polymer solution concentration and calculated cumulative production:

$$\Sigma(x - \bar{x})(y - \bar{y}) = (200 - 600)(118.44 - 122.81) + (400 - 600)(122.08 - 122.81) + (500 - 600)(123.54 - 122.81) + (600 - 600)(123.9 - 122.81) + (700 - 600)(123.9 - 122.81) + (800 - 600)(123.9 - 122.81) + (1000 - 600)(123.9 - 122.81) = 2584$$

Calculating the sum of the squares of the differences from the mean of polymer solution concentration and calculated cumulative oil production:

$$\Sigma(x - \bar{x})^2 = (200 - 600)^2 + (400 - 600)^2 + (500 - 600)^2 + (600 - 600)^2 + (700 - 600)^2 + (800 - 600)^2 + (1000 - 600)^2 = 420,000$$

Calculating the coefficients of the regression equation:

$$b = \Sigma(x - \bar{x})(y - \bar{y}) / \Sigma(x - \bar{x})^2 = 2,584 / 420,000 \approx 0.0062$$

$$a = \bar{y} - b * \bar{x} = 122.81 - (0.0062) * 600 \approx 119.1$$

The regression equation for polymer concentration ( $P_c$ ) and cumulative oil production volume ( $N_p$ ):

$$\text{Oil Production Volume } (N_p) = 119.1 + 0.0062 * P_c \dots\dots\dots 3(a)$$

Represented as  $A + B * P_c$  ..... 3(b) or for polymer solution viscosity ( $C_\mu$ ) is added to the equation.

$$N_p = C_\mu * A - B * P_c \dots\dots\dots 4$$

### Calculating the value of the correction factor $C_\mu$

The logarithm of viscosity ( $\text{Log}_{10}(\mu)$ ), and the logarithm of Buckley-Leverett calculated oil production volume ( $\text{Log}_{10}(N_p)$ ) were calculated. This transformation makes the relationship between x and y linear, then the slope of the regression line can be determined. Linear regression analysis was performed to find the correction factor:

### Calculating the mean values for $\text{log}_{10}(\mu)$ and $\text{log}_{10}(N_p)$ :

$$\text{log}_{10}(\mu) = (0.7782 + 1.1761 + 1.2718 + 1.3424 + 1.4698 + 1.5682 + 1.7076) / 7 \approx 1.3306$$

$$\text{log}_{10}(N_p) = (2.0735 + 2.0866 + 2.0918 + 2.0931 + 2.0931 + 2.0931 + 2.0931) / 7 \approx 2.0892$$



**Calculating the sum of the products of the differences from the mean for viscosity and cumulative production:**

$$\begin{aligned} \Sigma(\log_{10}(\mu) - \log_{10}(\bar{\mu}_1))(\log_{10}(N_p) - \log_{10}(N_{p1})) &= (0.7782 - 1.3306)(2.0735 - 2.0892) + \\ &+ (1.1761 - 1.3306)(2.0866 - 2.0892) + (1.2718 - 1.3306)(2.0918 - 2.0892) + (1.3424 - \\ &- 1.3306)(2.0931 - 2.0892) + (1.4698 - 1.3306)(2.0931 - 2.0892) + (1.5682 - 1.3306)(2.0931 - \\ &- 2.0892) + (1.7076 - 1.3306)(2.0931 - 2.0892) \approx \mathbf{0.0158} \end{aligned}$$

**Calculating the sum of the squares of the differences from the mean for each viscosity:**

$$\begin{aligned} \Sigma(\log_{10}(\mu) - \log_{10}(\bar{\mu}_1))^2 &= (0.7782 - 1.3306)^2 + (1.1761 - 1.3306)^2 + (1.2718 - 1.3306)^2 + (1.3424 - \\ &- 1.3306)^2 + (1.4698 - 1.3306)^2 + (1.5682 - 1.3306)^2 + (1.7076 - 1.3306)^2 \approx 0.5502 \end{aligned}$$

**Calculating the correction factor**

To take care of errors that may have arisen due to measurements, a correction factor is added to the model

$$b = \Sigma(\log_{10}(\mu) - \log_{10}(\bar{\mu}_1))(\log_{10}(N_p) - \log_{10}(N_{p1})) / \Sigma(\log_{10}(\mu) - \log_{10}(\bar{\mu}_1))^2 = 0.0158 / 0.5502 \approx 0.0287$$

Therefore, the correction factor for viscosity in the range of 1cp to 100cp is approximately 0.0287.

Estimating cumulative oil production based on viscosity in this range, the equation would be:

$$\text{Cumulative Oil Production Volume (Np)} = 10^{(2.0892 + 0.0287 * \log_{10}(\mu))}$$

$$\mathbf{Np = 10^{(2.0892 + 0.0287 * \log_{10}(\mu))} \dots\dots\dots 5}$$

Converting equation (4a) to natural logarithmic form based on the logarithm form by applying the conversion rule:  $\log a(b) = \ln(b) / \ln(a)$

Where:

$\ln()$  represents the natural logarithm

$$\text{Oil Production Volume (m}^3\text{)} = 10^{(a + b * \log_{10}(x))}$$

Applying this conversion to the logarithm form equation, with  $a = 2.0892$  and  $b = 0.0287$ :

$$\text{Oil Production Volume (m}^3\text{)} = 10^{(a + (b * \ln(x) / \ln(10)))}$$

Since  $\ln(10)$  is a constant value approximately equal to 2.3026, simplifying the equation:

$$\mathbf{(Np) = 10^{(a + (b * \ln(x) / 2.3026))} \dots\dots\dots 6}$$

Rewriting  $10^{(b * \ln(\mu_p) / 2.3026)}$  as  $e^{(b * \ln(\mu_p))}$

Since  $e^{(\ln(\mu_p))} = \mu_p$ :

Oil Production Volume ( $N_p$ ) =  $e^{((2.0892 * 2.3026 + 0.0287 * \ln(\mu_p)) / 2.3026)}$

.....7

$(N_p) = e^{((A * 2.3026 + B * \ln(\mu_p)) / 2.3026)}$  ..... 8

Where:

$e$  is the Euler's number (2.71828)

$A$  is 2.0892

$B$  is the correction factor (0.0287)

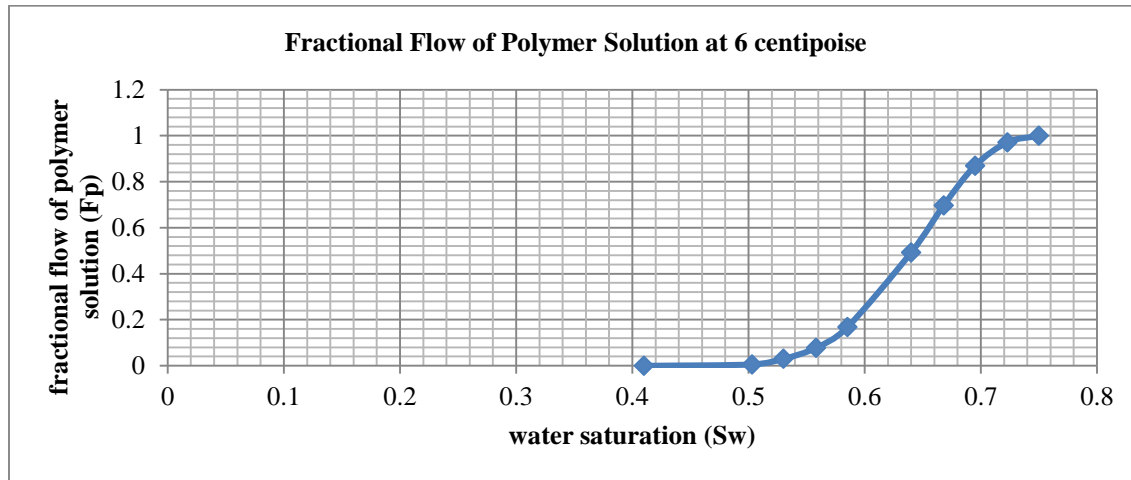
$\mu_p$  is polymer solution viscosity

This model is validated by comparing it to Buckley leverett model.

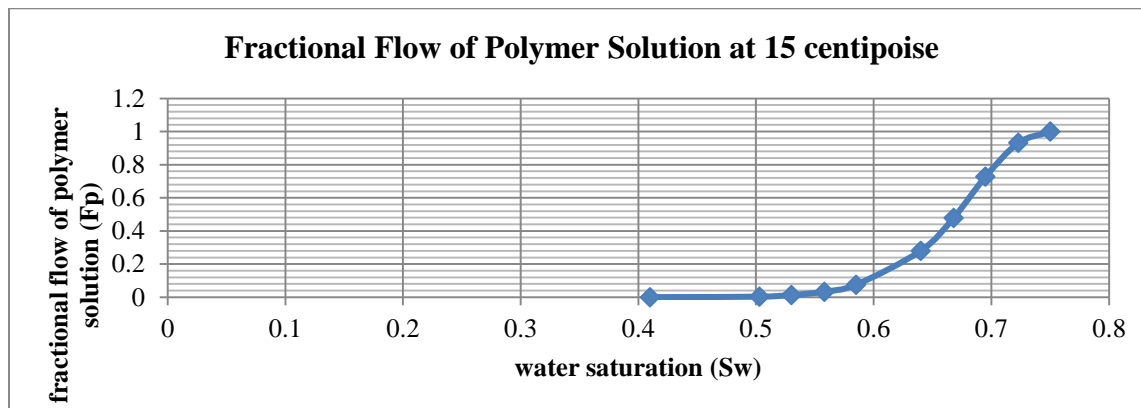
## RESULTS AND DISCUSSIONS

**Table 2 fractional flow of polymer solution at different viscosity**

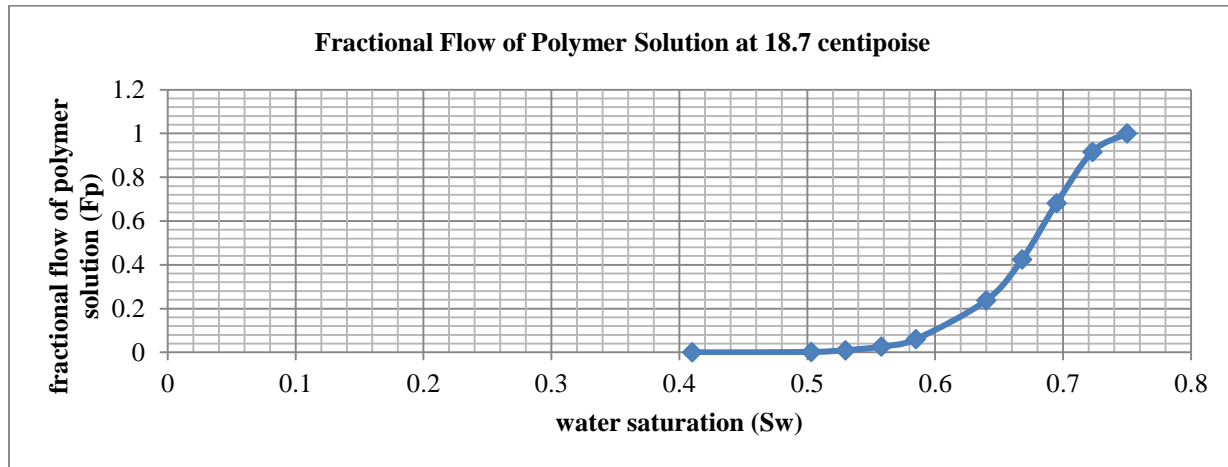
Sw	Kro	Krw	Fractional Polymer Solution Flow at different Viscosity						
			6 cp	15 cp	18.7 cp	22 cp	29.5 cp	37 cp	51 cp
0.410	1.000	0.000	0.0000	0.0000	0.0000	0.0000	0.0000	0.0000	0.0000
0.503	0.812	0.003	0.0061	0.0025	0.0019	0.0017	0.0013	0.0010	0.0007
0.530	0.643	0.012	0.0302	0.0123	0.0099	0.0084	0.0063	0.0050	0.0036
0.558	0.493	0.025	0.0779	0.0327	0.0264	0.0225	0.0169	0.0135	0.0098
0.585	0.364	0.044	0.1677	0.0746	0.0607	0.0521	0.0394	0.0316	0.0232
0.640	0.163	0.095	0.4927	0.2798	0.2376	0.1061	0.1650	0.1361	0.1026
0.668	0.092	0.127	0.6971	0.4792	0.4247	0.3855	0.3188	0.2717	0.2130
0.695	0.041	0.164	0.8696	0.7273	0.6814	0.6452	0.5755	0.5195	0.4396
0.723	0.010	0.205	0.9715	0.9318	0.9164	0.9031	0.8742	0.8471	0.8008
0.750	0.000	0.251	1.0000	1.0000	1.0000	1.0000	1.0000	1.0000	1.0000



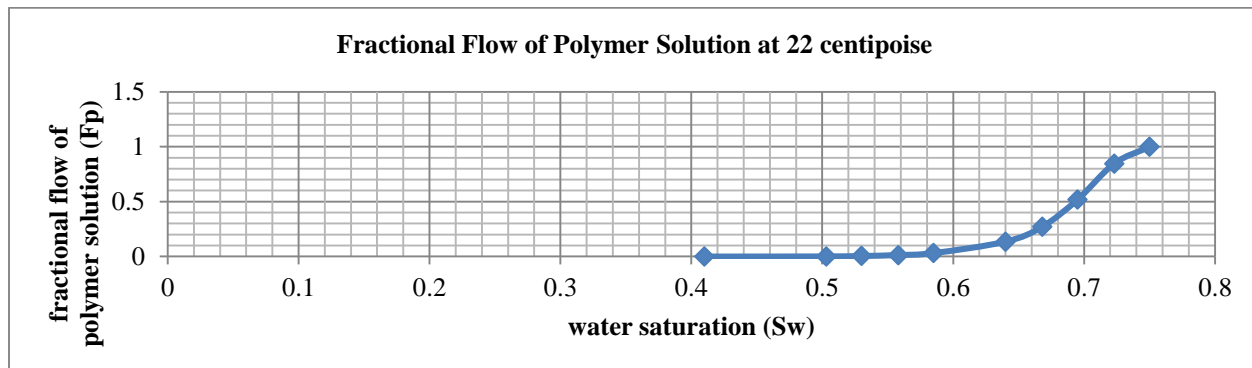
Graph 1.S-curve for polymer solution fractional flow at 6 centipoise



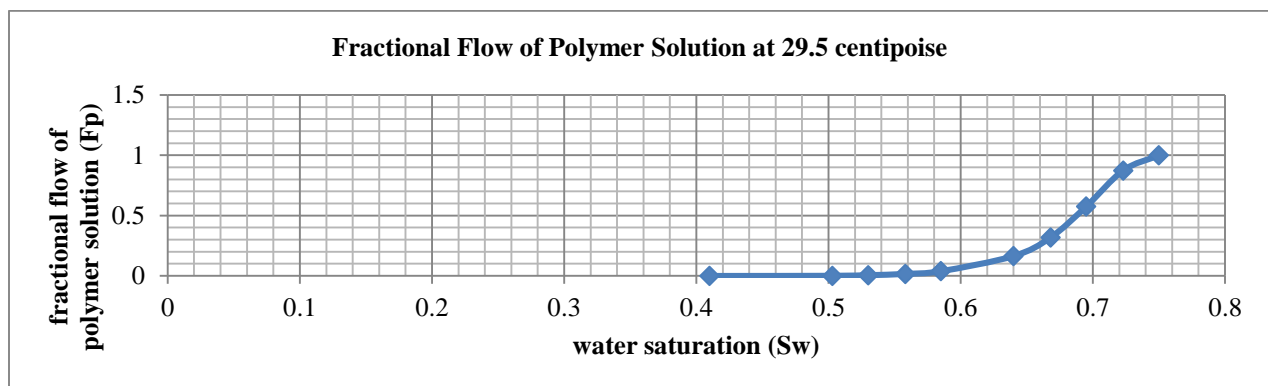
Graph 2. S-curve for polymer solution fractional flow at 15 centipoise



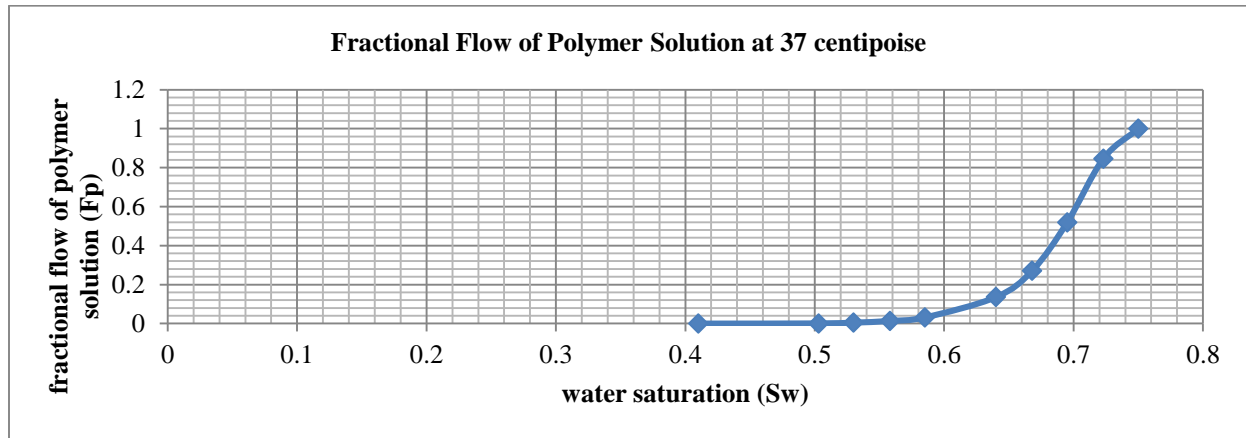
Graph 3. S-curve for polymer solution fractional flow at 18.7 centipoise



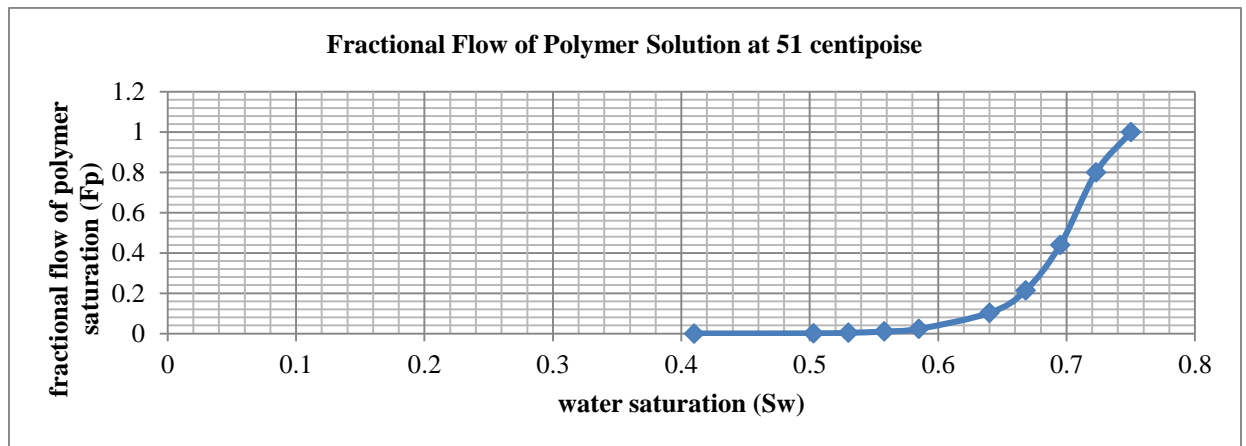
Graph 4. S-curve for polymer solution fractional flow at 22 centipoise



Graph 5 S-curve for polymer solution fractional flow at 29.5 centipoise



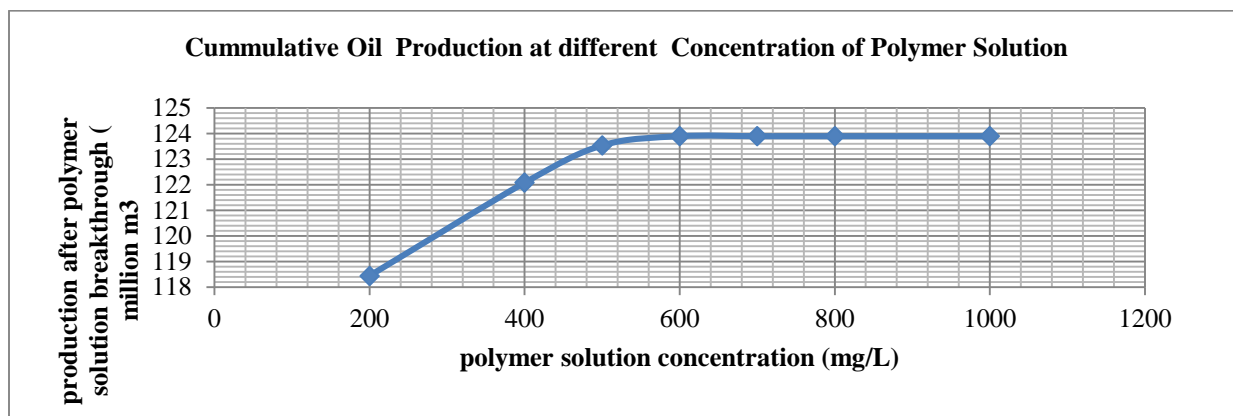
Graph 6 S-curve for polymer solution fractional flow at 37 centipoise



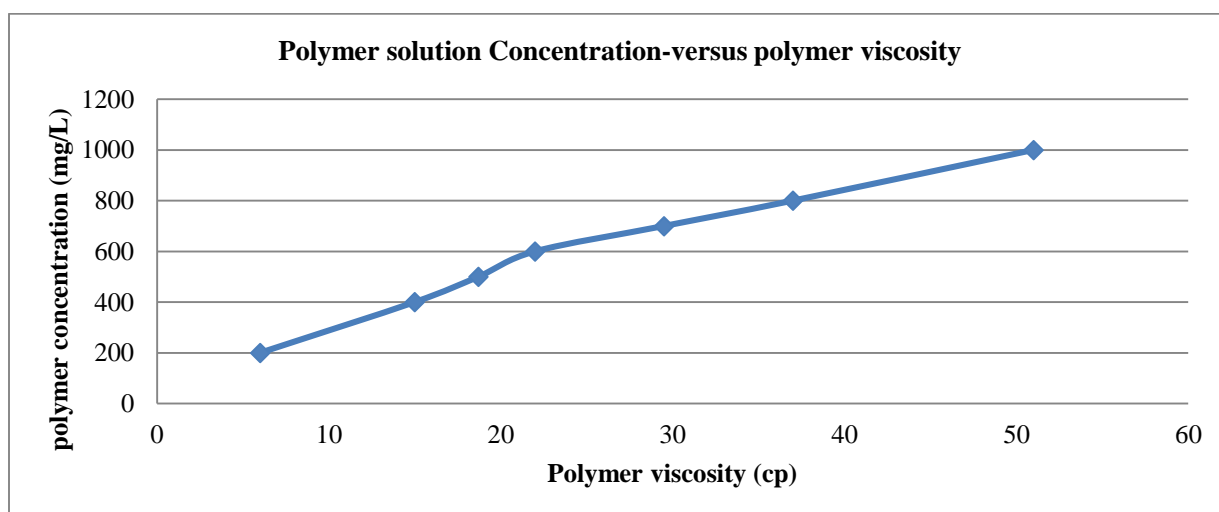
Graph 7 S-curve for polymer solution fractional flow at 37 centipoise

Table 3. cumulative oil production at different viscosity of polymer solution

Polymer Solution Viscosity( cp)	Polymer Solution Concentration ( mg/L)	Oil Production after Breakthrough. (Million m <sup>3</sup> )
6	200	118.44
15	400	122.08
18.7	500	123.54
22	600	123.90
29.5	700	123.90
37	800	123.90
51	1000	123.90



Graph 8 Cumulative Oil Production at different Viscosity of Polymer Viscosity



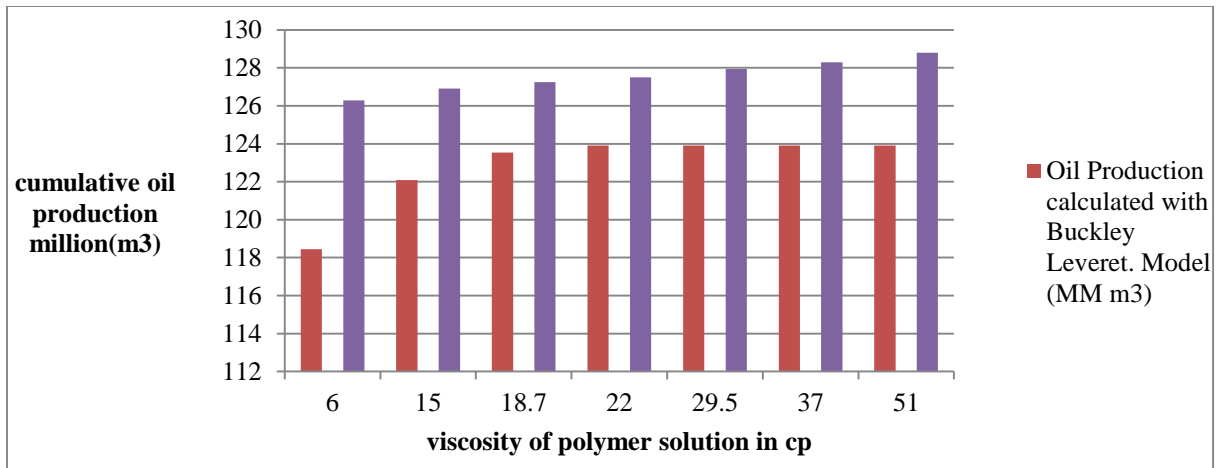
Graph 9. Polymer solution concentration versus polymer solution viscosity

Table 4. Logarithm of viscosity and Buckley-Leverett calculated cumulative oil production

Viscosity ( $\mu$ ) cp	Cumulative oil Production ( $N_p$ ) MM m <sup>3</sup>	Log10( $\mu$ )	log10( $N_p$ )
6	118.44	0.7782	2.0735
15	122.08	1.1761	2.0866
18.7	123.54	1.2718	2.0918
22	123.90	1.3424	2.0931
29.5	123.90	1.4698	2.0931
37	123.90	1.5682	2.0931
51	123.90	1.7076	2.0931

Table. 5. Cumulative Oil production calculated with Buckley Leverett Model versus cumulative oil production estimated with Developed Model

Polymer viscosity cp	6	15	18.7	22	29.5	37	51
Oil Production calculated with Buckley Leveret. Model (MM m <sup>3</sup> )	118.44	122.08	123.54	123.90	123.90	123.90	123.90
Oil Production Estimated with Developed Model (MMm <sup>3</sup> )	126.29	126.91	127.24	127.50	127.94	128.29	128.79
Percentage Error (%)	6.63	3.96	2.99	2.91	3.26	3.54	3.95



Graph. 10. Cumulative Oil production calculated with Buckley-Leverett Model versus cumulative oil production estimated with Developed Model

## DISCUSSION

Buckley-Leverett Model is a simplified, one-dimensional, two-phase flow model. It assumes that the oil and water phases have constant properties and that there is no dispersion or diffusion between the phases.

Table 1: The Fractional Polymer Solution Flow at Different Viscosity presents the fractional flow of polymer solution at various viscosity. The data shows that as viscosity increases, the fractional flow decreases. This is expected, as higher viscosity fluids are more resistant to flow.

Graphs 1-7: S-Curves for Polymer Solution Fractional Flow illustrate the S-curve relationship between polymer solution fractional flow and viscosity. Each graph represents a different viscosity value. The S-curve shape indicates that the fractional flow increases rapidly at low viscosity and then levels off at higher viscosity.



Table 3: Cumulative Oil Production at Different Viscosity of Polymer Solution presents the cumulative oil production at different viscosity of polymer solution. The data shows that oil production prediction with Buckley-Leverett model increases with viscosity ( $\mu_p$ ) to a certain point (around 22 cp) and then remains constant.

Graph 9: Polymer Solution Concentration versus Polymer Solution Viscosity shows the relationship between polymer solution concentration and viscosity. The graph indicates a positive correlation between the two variables.

Table 4: Logarithm of Viscosity and Buckley-Leverett Calculated Cumulative Oil Production presents the logarithm of viscosity and the corresponding cumulative oil production calculated using the Buckley-Leverett model. The data shows a linear relationship between the logarithm of viscosity and cumulative oil production.

Table 5: Cumulative Oil Production Calculated with Buckley-Leverett Model versus Cumulative Oil Production Estimated with Developed Model compares the cumulative oil production calculated using the Buckley-Leverett model with the estimated values using a developed model. The data shows that the developed model estimates higher oil production values, with a percentage error ranging from 2.91% to 6.63%. the lowest percentage error corresponded with polymer solution concentration of 600mg/L, this indicates an optimum polymer concentration and oil recovery using the developed model in prediction.

Graph 10: Cumulative Oil Production Calculated with Buckley-Leverett Model versus Cumulative Oil Production Estimated with Developed Model illustrates the comparison between the cumulative oil production calculated using the Buckley-Leverett model and the estimated values using the developed model. The graph shows that the developed model estimates higher oil production values, with a increasing trend.

The results have demonstrated that in the xanthan polymer flooding process, increases in polymer solution concentration do not necessarily yield increases in cumulative oil production because the highest polymer solution concentration may not translate to higher oil production, therefore an optimum or critical polymer concentration is necessary. In this research, a polymer concentration of 600mg/L gave the highest cumulative oil production of 123.90 MMm<sup>3</sup> of oil. Further, an increase in the polymer concentration above 600 mg/L did not yield more oil

production because adsorption of the polymer by the porous medium may have resulted due to the polymer solution concentration being too high. This can lead to the formation of channels within the reservoir known as polymer wormholes. These channels can bypass the oil zones resulting in less contact between the injected polymer solution and oil.

Another reason why a higher concentration of polymer solution did not yield further increment in oil production may be because high polymer concentrations can cause gel-like structures within the pores of the reservoir thereby acting as a barrier, trapping oil and preventing its mobilization towards the production wells. An unstable flow pattern can result from flooding with a higher concentration of polymer solution leading to uneven sweep efficiency.

Since the Model is a derivative of the Welge-modified Buckley–Leverett equation, it has been validated by this process of derivation.

## CONCLUSION

From the research, conclusions can be drawn as follows;

The developed Mathematical model is for a light oil, and medium oil reservoir with a viscosity range of 1cp to 100 cp (48.4 -28.4 API gravity). Polymer flooding is a very effective recovery method in enhanced oil recovery and its success is partly mostly dependent on polymer solution concentration.

It is very important to optimize the polymer concentration during polymer flooding to eliminate the adverse effect and conserve resources. This simplistic Model can serve as a firsthand tool in achieving this objective.

The developed prediction model for polymer flooding estimates higher oil production compared to the Buckley-Leverett model, especially at higher polymer viscosity. This suggests that the developed model can better capture the effects of polymer viscosity due to polymer concentration on oil displacement efficiency.

## REFERENCE

- [1] Wang, D (2013), Enhanced oil recovery field case studies chapter 4 pages 83-116.
- [2] Jacobsen, J., Alzaabi, M., Tormod, S., Sorbie, K., Skauge, A., 2019 Analysis and Simulation of polymer injectivity. In: IOR 2019- 20<sup>th</sup> European Symposium on Improved Oil Recovery
- [3] Rego, F.B, Botechia, V.E, Schiozer, D.J 2017 Heavy oil recovery by polymer flooding and hot water injection using numerical simulation. Journal of Petroleum Science and Engineering volume 153, pages 187 – 196
- [4] Jain, L and Lake, L.W Surveillance of secondary and tertiary floods: Application of Koval's theory to isothermal enhanced oil recovery displacement. SPE Improved Oil Recovery Symposium, Society of Petroleum Engineers (2014)
- [5] Abdelaziz el-hoshoudy (2024). Mathematical prediction of oil recovery factor for nano particles assisted polymer flooding through statistical analysis and ANN Modeling. . 4<sup>th</sup> international conference of applied chemistry, July 2024
- [6] Imankulov, T., Kenzhebek, Y., Bekele, S.D., Makhmut, E 2024. enhancing oil recovery prediction by leveraging polymer flooding simulations and machine learning models on a large synthetic data-set. Energies, vol17, issue 14, pp. 3397

- [7] Keith, C.D., Wang, X; Zhang, Y; Dandekar, A.Y; Ning, S; Wang, D 2022 oil recovery prediction for polymer flood field test of heavy oil on Alaska North Slope via machine assisted reservoir simulation. Paper presented at the SPE Improved oil recovery conference, April 2022. paper number: SPE-209443-MS
- [8] Hassan, A.M., Al-Shalabi, E.W., Alameri, W., Kamal, M.S., Patil, S., and Hussain, S.M.S.(2023). Manifestations of surfactant-polymer flooding for successful field applications in carbonates under harsh conditions: A comprehensive review. *Journal of Petroleum Science and Engineering*, 220, 111243.
- [9] Li, Z., Dean, R.M., Lashgari, H., Luo, H., Driver, J.W., Winoto, W., and Pin, E. (2024). Recent advances in Modeling Polymer Flooding. In *SPE Improved Oil Recovery Conference*
- [10] Salih, T.A., Sahi, S.H., and AL-Dujaili, A.N.G. (2016) Using different surfactants to increase oil recovery of Rumaila field (Experimental Work). *Iraqi Journal of Chemical and Petroleum Engineering*, 17(3), 11-31
- [11] Seright, R.S., and Wang, D. (2023) Polymer flooding: Current status and future directions. *Petroleum Science*, 20(2), 910-921
- [12] Zeynalli, M., Mushtag, M., Al-Shalabi, E.W., Alfazazi, W.(2023). A comprehensive review of viscoelastic polymer flooding in sandstone and carbonate rocks. *Scientific Reports*, 13(1), 17679
- [13] Xiangji Dou, An Wang, Shikai Wang, Dongdong Shao, Guoqiang Xing, and Kun Qian 2022 study the viscosity optimization of polymer solutions in a heavy oil reservoir based on process simulation. *Energies*, volume 15 issue 24, page 9473.
- [14] Sharafi, M.S.; Jamialahmadi, M.; Hoseinpour, S.-A. Modelling of viscoelastic polymer flooding in Core-scale for prediction of oil recovery using a numerical approach. *J. Mol. Liq.* 2018, 250, 295–306
- [15] Flory, P.J (1953) *Principles of Polymer chemistry* cornel university press, Ithaca
- [16] Ahmed Ali Manzoor 2020 Modeling and Simulation of Polymer flooding with time-varying injection pressure. *ACS Omega* volume 5, issue 10, pages 5258 -5269
- [17] Chauhuri, A and Vishnudas, R. (2018) A systematic numerical modeling study of various polymer injection conditions on immiscible and miscible viscous fingering and oil recovery in a five-spot setup. *Fuel*, volume 232, november 2018pp. 431-443
- [18] Davarpanah, A and Mirshekari B. (2019) A mathematical model to evaluate the polymer flooding performances *Energy Reports* volume 5, 2019, pages 1651-1657
- [19] Wang, J.; Liu, H. A novel model and sensitivity analysis for viscoelastic polymer flooding in offshore oilfield. *Journal of Industrial and Engineering Chemistry*. 2014, volume 20, issue 2, pages 656–667.
- [20] Zamani, N.; Bondino, I.; Kaufmann, R.; Skauge, A. Computation of polymer in-situ rheology using direct numerical simulation. *J. Pet. Sci. Eng.* 2017, 159, 92–102
- [21] Francisco Javier Rosado-Vazquez et al, 2023 Compositional streamline-based modelling of polymer flooding including rheology, retention, and salinity *ACS Omega*, volume 8 issue 40, pages 36948 – 36965
- [22] Xiankang Xin, Gaoming Yu, Keliu Wu, Xiaohu Dong, and Zhangxin Chen 2021 Polymer Flooding in Heterogeneous Heavy Oil Reservoirs: Experimental and Simulation Studies *Polymers* 2021, 13, 2636.
- [23] Wenyue, Z; Huo, T; Fan, L; Shuai, H; Tongjing, L; Nannan, L; and Renzhi, S . Mathematical model for oil recovery prediction of polymer microsphere conformance control based on the stream tube method. *Materials* 2023 16(4). 1476

[24] Buckley, S.E and Leverett, M.C (1942) Mechanism of fluid displacement in sands . Trans. 146 (01): 107-116 Paper number:SPE942107-G

## Appendix

### Nomenclature

A	Area
Bo	Oil formation volume factor
Cp	Centipoise
Fp	Fractional flow of polymer
Kro	oil relative permeability
Krw	water relative permeability
L	Length
m	Meter
Mg	milligram
Mg/L	milligram/liter
MM	.million
NpI	.mean cumulative oil production
Np	cumulative oil production
oC	.degrees Celsius
oF	.degrees Fahrenheit
Pc	polymer solution concentration
μo	Oil viscosity
μw	Water viscosity
μI	mean viscosity
Swbt	Water saturation at breakthrough
Sw	water saturation
%	Percentage
Φ	Porosity